Physicochem. Probl. Miner. Process., 62(6), 2026, 242827

http://www.journalssystem.com/ppmp

Physicochemical Problems of Mineral Processing

ISSN 1643-1049
© Wroclaw University of Science and Technology

Particle size effects and Weibull statistical characterization of fracture behavior in multi-component phosphate ore

Runzhe Liu [1], Jun Ren [2], Mengtao Wang [2], Qingfei Xiao [2], Menglai Wang [1], Lingpan Du [1], Saizhen Jin [2]

[1] Yunnan phosphate chemical group Co., Ltd.

[2] Faculty of Land Resources Engineering, Kunming University of Science and Technology, Kunming 650093, Yunnan, China

Corresponding author: wang.mt@foxmail.com (Mengtao Wang)

Abstract: In this study, uniaxial compression tests were conducted on quartz, dolomite, apatite, and phosphate ore to analyze the fracturing behavior of pure minerals and actual ores under different particle size conditions. The fracturing characteristics were characterized using the Weibull distribution model. Experimental results indicate that for pure mineral specimens, the distributions of σ0 and m are relatively concentrated, and their fracturing behavior is relatively regular, primarily governed by the intrinsic mechanical properties of the minerals. In contrast, due to the influence of multi-mineral distribution, mineral interfaces, and structural defects, the distributions of σ0 and m in actual ores exhibit more pronounced dispersion, and their fracturing behavior gradually deviates from the characteristics typically observed in single-mineral specimens. As particle size increases, structural heterogeneity in actual ore gradually becomes the dominant factor, manifesting as a decrease in characteristic strength and Weibull modulus, as well as increased variability in crushing behavior; this scale effect is relatively weak in pure minerals. Studies indicate that σ0 and m are not fixed material constants, but rather statistical parameters that evolve with changes in particle size. These findings provide experimental support for modeling the crushing and grinding processes of multi-component ores and for the scale correction of strength parameters.

Keywords: multi-component ore, uniaxial compression, Weibull distribution, characteristic strength, size effect

1. Introduction

Crushing and grinding are among the most energy-intensive operations in mineral processing, directly influencing resource utilization efficiency and production cost (Somani, Nandi, Pal, Majumder, 2017). During comminution, single-particle breakage represents the fundamental mechanical unit. The breakage mode directly affects ore liberation and energy utilization efficiency (Zong-Xian et al., 2023). The mechanical response at the particle scale provides a critical basis for understanding macroscopic comminution processes, highlighting the need for in-depth analysis of breakage behavior and its controlling mechanisms. Particle fracture behavior is influenced by a combination of factors, including the inherent properties of the mineral itself, as well as particle size and internal structure. The strength of a mineral is governed by its crystal structure, bonding characteristics, and defect distribution. These factors determine the fundamental strength level of the material. Changes in particle size introduce a size effect, causing strength to decrease systematically as particle size increases. At the same time, natural ores typically consist of multiple minerals, exhibiting complex intergrowth structures, mineral interfaces, and networks of microcracks. This structural heterogeneity alters stress distribution and crack propagation behavior, leading to increased variability and discontinuity during the particle fragmentation process.

It is important to distinguish the two mechanisms. In a homogeneous material the size effect is essentially statistical: a larger specimen has a higher probability of containing a critical flaw, so that strength decreases with size under the weakest-link assumption, and the local stress concentration is

DOI: 10.37190/ppmp/242827

governed by the geometry of the individual flaws. In a multi-component ore an additional mechanism operates. The constituent minerals differ in elastic modulus, hardness and fracture toughness, so that the stress field is redistributed at phase boundaries: the stiffer or stronger phase carries a larger share of the load, while the softer phase and the interface region experience locally amplified stress. Size and heterogeneity therefore act jointly rather than independently. Increasing particle size raises not only the number of potential flaws but also the number and total area of mineral interfaces, and each interface acts as an additional stress concentrator. The two effects reinforce each other: the flaw population determines where cracks can initiate, whereas the interfaces determine how strongly the local stress is amplified and how the crack is deflected. This coupling is absent in homogeneous materials and explains why the strength scatter and its size dependence are more pronounced in multi-component ores.

Previous research has extensively investigated particle fragmentation and size effects. Studies have shown that the strength of brittle materials decreases as particle size increases; this relationship is typically described by a power-law function (Armstrong, 2019; Tavares, 2022). Based on the theory of the weakest link, the strength distribution of particles is often assumed to follow a Weibull distribution, where the characteristic strength σ_0 reflects the strength level and the modulus m describes the degree of dispersion (Bertalan et al., 2014). Most existing studies focus on single minerals or homogeneous materials, and there is a lack of systematic analysis regarding the coupled effects of structural heterogeneity and size effects in multi-component ores. The four size classes (6.5–22 mm) span the range over which the size effect governs both the crushing force and the mineral liberation of phosphate ore in industrial comminution and thus allow the size dependence of the Weibull parameters to be resolved.Uncertainty remains regarding whether Weibull parameters vary with particle size. In particular, within multi-component ore systems, the coupling mechanisms among mineral crystal structure characteristics, size effects, and structural heterogeneity remain unclear (Li, Xiao, Fu, Jin, Wang, Wang, Sun, Tian, Liu, Tian, 2025), and there is still a lack of systematic understanding regarding their impact on particle fragmentation behavior and its statistical patterns (Unland and Al-Khasawneh, 2009; Dyskin and Pasternak, 2020).

Phosphate ore is a key raw material for the phosphate chemical industry (Budemberg et al., 2025). It typically consists of minerals such as apatite, dolomite, and quartz, and exhibits distinct heterogeneous characteristics in its internal structure. Before it can be converted into phosphoric acid and phosphate fertilizers, phosphate ore must undergo crushing, grinding, and downstream beneficiation, in which flotation is the dominant separation method. The crushing and grinding stages largely determine both the energy cost and the quality of the subsequent beneficiation: the particle size distribution and the degree of liberation of apatite from its gangue directly control the grade and recovery of the flotation concentrate. Because apatite, dolomite, and quartz have similar surface properties, insufficient liberation leaves locked particles that depress concentrate grade, whereas excessive grinding produces fine slimes that consume reagents and reduce flotation selectivity (Yang, Li, He, Gong, Xu, Zhu, Zhu, Zhang, 2026; Chen, Zhang, Xiong, Zhu, Chen J., 2026). The breakage mode and the size effect therefore jointly determine mineral liberation and energy consumption in the downstream grinding–beneficiation chain. However, this multi-component embedded structure causes the crushing behavior of phosphate ore to differ from that of single-mineral systems (Alona and Daniel, 2018; Lois-Morales et al., 2022), making models based on pure minerals difficult to apply directly to actual ores (Budemberg et al., 2025). Phosphate ore differs from most ores in two respects that bear directly on comminution. First, it combines minerals with strongly contrasting mechanical properties—quartz (Mohs 7), apatite (Mohs 5) and dolomite (Mohs 3.5–4)(Klein & Dutrow, 2007)—so that stress is partitioned non-uniformly among the mineral phases and fracture tends to follow the weaker phases and the interphase boundaries. Second, the valuable mineral (apatite) and the principal carbonate gangue (dolomite) are both calcium-bearing salt-type minerals with similar surface chemistry, so that their flotation separation depends critically on the degree of liberation achieved during comminution. Together with the fine, cryptocrystalline intergrowth of collophane, these features make the breakage behaviour of phosphate ore fundamentally different from that of homogeneous single minerals (Armstrong, 2019; Tavares, 2022), on which most existing breakage models are based.Quantifying single-particle breakage in

phosphate ore is therefore a prerequisite for optimizing the crushing–grinding–beneficiation chain, which is of clear practical significance.

This study conducted a systematic investigation of phosphate ore and its constituent minerals through single-particle compression tests. It analyzed the variation of maximum crushing force and fracture strength with particle size and applied the Weibull model to characterize the strength distribution. XRD techniques were used to correlate crystal structure characteristics with mechanical behavior. This study aims to reveal the scale dependence of Weibull parameters (σ_0 and m) in multicomponent systems and to elucidate the coupled effects of size effects and structural heterogeneity in determining particle fracture behavior. In contrast to previous studies that focused on single minerals or homogeneous materials, this work (i) compares the single-particle breakage of a multi-component phosphate ore with that of its constituent minerals under identical loading conditions, (ii) links the resulting strength statistics to crystal-structure information, and (iii) quantifies the size dependence of the Weibull parameters in a genuinely heterogeneous system. This extends the Weibull-based description of strength scaling from homogeneous materials to multi-component ores and provides a basis for evaluating selective comminution and over-grinding in phosphate beneficiation.

2. Experimental materials and protocols

2.1 Experimental materials and equipment

A YCAW-300F microcomputer-controlled electronic compression testing machine was used. primarily to measure the maximum crushing force and deformation of irregular ore particles. The system can apply a maximum axial pressure of 300 kN. The force measurement accuracy is approximately 1%. The minimum displacement rate of the loading plate is 2 mm/min, and the maximum travel speed is 30 mm/min. The YCAW-300F microcomputer-controlled electronic pressure testing machine and the loading experimental setup are shown in Fig. 1(a).

The mineral samples tested included pure minerals such as quartz, dolomite, and apatite, as well as phosphate ore, as shown in Fig. 1 (b). The pure mineral samples were obtained through manual sorting, and their purity was confirmed to be above 90% via XRD analysis. Quartz consists primarily of SiO_2 and has a silicate tetrahedral framework crystal structure; dolomite is a magnesium-calcium carbonate mineral with the chemical formula $CaMg(CO_3)_2$, and a rhombohedral crystal structure; apatite is the primary useful mineral in phosphate ore, with the theoretical chemical formula $Ca_5(PO_4)_5(F, Cl, OH)$ and a hexagonal crystal system. Phosphate ore is a multi-mineral disseminated system, primarily composed of minerals such as apatite, dolomite, and quartz. For this experiment, irregular ore samples were selected in four particle size fractions with geometric mean diameters of 5–8 mm, 8–12 mm, 12–19 mm, and 19–25 mm.



Fig. 1 Experimental setup (a) and ore specimens (b)

2.2. Test plan

2.2.1. Test method

Irregular particles of quartz, dolomite, apatite, and phosphate ore were placed on the loading of the compression testing machine with their short axes aligned with the axial direction, ensuring that the

center of the loading plate coincides with the center of gravity of the specimen. First, the load was applied at a higher displacement rate until the loading plate approached the particles. The displacement rate was then reduced until the upper loading plate just contacted the particles. Subsequently, the relevant parameters were set, such as the loading rate, on the control panel. The loading rate for this experiment was set at 2 mm/min, which is the minimum displacement rate of the testing machine, so as to approximate quasi-static loading and to minimize rate-dependent and inertial effects. The ore samples were divided into four particle size ranges: 5–8 mm, 8–12 mm, 12–19 mm, and 19–25 mm., with each range comprising four different types of ore. During the test, a uniform load was applied to the samples using a pressure testing machine, and the loading process began; simultaneously, the pressure and deformation data were automatically recorded throughout the loading process. Complete fracture is defined as: the original specimen has split into multiple separate fragments, and the axial force has dropped abruptly to a residual value close to zero, such that the specimen can no longer withstand the applied load. Therefore, loading is terminated when such an abrupt drop occurs in the force-displacement curve, or when the specimen visibly fractures into multiple separate fragments (whichever occurs first). The peak force prior to this abrupt drop is considered the maximum crushing force. A particle was regarded as completely fragmented when its largest remaining fragment was reduced to one-third or less of its original diameter. Since the loading device of this testing system has a high load-bearing capacity, the effect of the device's own deformation on the test results can be neglected. For this experiment, 20 replicate tests were conducted for each particle size fraction of each ore type; with four particle size fractions set for each ore type, a total of 80 test sets were performed; for the four ore types combined, a total of 320 test sets were completed.

Material strength is defined by its ability to resist external forces or energy input, which is fundamentally governed by the bonding state between internal particles. The intrinsic nature of strength is closely related to the type of chemical bonds and their mechanical properties. In this study, three parameters are used to characterize the strength of irregular ore particles: maximum breakage force, fracture energy, and breakage strength. The maximum breakage force represents the highest load that a single particle can sustain in one loading event before fracture, i.e., its ultimate load-bearing capacity for a single fracture, rather than the bulk strength of the material. Fracture energy refers to the energy absorbed during the fracture process (Bertalan, Shekhawat, Sethna, Zapperi, 2014), indicating the material's resistance to crack propagation and failure. Breakage strength denotes the resistance exhibited by a material at the point of failure under applied load or stress and is commonly used to describe its compressive or tensile strength. Previous studies have demonstrated that the maximum crushing force Fgenerally follows a power-law relationship with particle size D. This relationship can be described using the single-particle crushing model (Tavares, 2022), which is a typical empirical expression of the size effect widely applied in materials science, fracture mechanics, and geotechnical engineering. A related scaling is given by the generalized energy–size law (Hukki, 1961), in which φ = 1, 0.5 and 0 correspond to the Rittinger, Bond and Kick laws, respectively. The corresponding relationship is expressed in Eq. (1):

$$E \propto \left(\frac{d_0}{d_\mathrm{p}}\right)^{\varphi} \tag{1}$$

The power-law relationship between fracture force and particle size originates from the statistical distribution of internal defects and the associated stress concentration mechanisms within particles. Previous studies have further shown that fracture energy also follows a similar power-law relationship with particle size, supporting the applicability of this model for describing particle fracture behavior (Tavares, 2022; Li, Xiao, Fu, Jin, Wang, Wang, Sun, Tian, Liu, Tian, 2025). Accordingly, the maximum crushing force of a single particle follows an empirical power-law relation with particle size:

$$F = aD^b \tag{2}$$

In the equation, E corresponds to the material's elastic modulus, fracture energy, or strength; d_0 corresponds to the characteristic dimensions of the material's microstructure (such as particle diameter or particle size); d_p corresponds to the macroscopic specimen dimensions or defect dimensions; and φ corresponds to the size effect exponent (typically a positive number), which reflects the extent to which changes in size affect E, F represents the maximum breakage force of irregular ore particles (kN), D

denotes particle size (mm), and a and b are are fitting parameters determined from the experimental data of this study.

The characteristic strength derived from the Weibull distribution scales with particle size as (Weibull, 1951):

$$\sigma \propto D^{-1/m} \tag{3}$$

where m is the Weibull shape parameter (modulus); the exponent −1/m reflects the scaling of the critical-flaw population with particle size and is tested against the experimental data in Section 3. The size dependence of the fracture strength is then described by a power law (Armstrong, 2019; Tavares, 2022):

$$\sigma = aD^{-b} \tag{4}$$

where σ corresponds to the fracture strength of irregular ores, MPa; D Corresponding size of particles, mm; m is the shape parameter; a and b are the parameters in the equation.

2.2.2. Weibull distribution model

Subsequent theoretical analysis indicates that the fracture strength of particles typically follows a Weibull distribution. Related studies have shown that the two-parameter Weibull distribution model provides a good fit for the experimental data of most irregular ores (Bertalan, Shekhawat, Sethna, Zapperi, 2014). Therefore, the two-parameter Weibull distribution model was adopted and uses the cumulative distribution function to describe the fracture characteristic strength of various types of irregular ores under different particle size conditions. The cumulative failure probability of a particle is described by the two-parameter Weibull distribution (Weibull, 1951):

$$P(\sigma) = 1 - \exp\left[-\left(\frac{\sigma}{\sigma_0}\right)^m\right] \tag{5}$$

Equation (6) is obtained by rearranging Eq. (5):

$$1 - P = \exp\left[-\left(\frac{\sigma}{\sigma_0}\right)^m\right] \tag{6}$$

Taking the natural logarithm of Eq. (6) gives Eq. (7):

$$\ln\frac{1}{1-P} = \left(\frac{\sigma}{\sigma_0}\right)^m \tag{7}$$

Taking the logarithm once more yields the linearized form, Eq. (8):

$$\ln\left[\ln\frac{1}{1-P}\right] = m\ln\sigma - m\ln\sigma_0 \tag{8}$$

The probability that a particle survives under a given stress is given by the Weibull survival function, with the nominal stress defined as $\sigma = F_B/d^2$ (Weibull, 1951; Hiramatsu and Oka, 1966):

$$P_S = \exp\left[-\left(\frac{F_B}{d^2\sigma_0}\right)^m\right] \tag{9}$$

Combining Eqs. (5)–(9), gives, gives the two-parameter Weibull model, Eq. (10):

$$\ln\ln\frac{1}{P_S} = m\ln\frac{F_B}{d^2} - m\ln\sigma_0 \tag{10}$$

In the equation, $P(\sigma)$ is the failure probability, σ is the stress, P_S represents the cumulative survival probability. F_B represents the maximum test force (N), d denotes the initial particle diameter, which is defined as the distance between the two loading contact points (mm), m represents the Weibull distribution modulus; and σ_0 represents the characteristic strength of the irregular ore (Mpa).

As shown in Eq. (10) and Ref. (Bertalan, Shekhawat, Sethna, Zapperi, 2014), the Weibull modulus can be calculated simply by determining the stress σ of the irregular ore and the corresponding cumulative survival probability P_S. By performing a linear fit on the data points for stress and cumulative survival probability using Eq. (10), the slope of the line is m and the y-intercept is $-m\ln\sigma_0$. From the y-intercept, we can calculate the characteristic strength σ_0 of the irregular ore particles.

2.2.3. Selection of particle size fractions

Four particle size classes were adopted in this study. The size range (nominal 6.5–22 mm, corresponding to the sieve fractions from −25+19 to −8+5 mm) was chosen because it covers the coarse-crushing

product and grinding-feed sizes of phosphate ore, over which the size effect on single-particle strength most strongly influences downstream liberation and comminution energy. Six standard sieve fractions were initially prepared. To ensure a statistically robust number of particles for the Weibull analysis while retaining four size levels that span the range, two pairs of adjacent intermediate fractions (−19+15 with −15+12 mm, and −12+10 with −10+8 mm) were merged, giving four classes with nominal sizes of 22, 15.5, 10 and 6.5 mm and n = 20, 40, 40 and 20 particles, respectively. Four levels were selected because the two-parameter power law (Eq. 4) contains two unknowns and therefore requires at least four levels to test its adequacy, while the largest-to-smallest size ratio of ≈3.4 provides sufficient leverage to resolve the exponent. Additional fractions would multiply the number of single-particle tests without materially improving the resolution of the size effect. Within each class the particles are confined to a narrow sieve interval rather than spanning a continuum, and the residual variability among individual particles is not treated as noise: it is quantified through the Weibull modulus m, which is one of the main quantities analyzed in this study. In this sense, the within-fraction variability is the object of the analysis rather than a confounding factor.

3. Results and discussion

3.1 Size effect in particle crushing

Table 1. Summary of single-particle compression results for phosphate ore and its constituent

Mineral	Size class	n	d(mm)	F_{max}(kN)	σ(MPa)
Quartz	22	20	23.58	5.78±1.76	8.97±2.20
	15.5	40	18.28	3.43±0.57	9.14±1.31
	10	40	12.15	1.73±0.23	11.24±1.86
	6.5	20	9.27	1.24±0.18	13.42±2.35
Dolomite	22	20	24.96	2.42±0.44	5.50±1.11
	15.5	40	18.16	1.27±0.23	6.78±1.37
	10	40	11.60	0.56±0.13	7.93±1.83
	6.5	20	9.13	0.39±0.10	10.00±3.18
Apatite	22	20	30.33	4.59±1.33	4.40±1.11
	15.5	40	17.94	2.02±0.41	5.62±0.96
	10	40	11.51	1.03±0.22	6.90±1.39
	6.5	20	8.19	0.51±0.18	7.38±3.57
Phosphate Ore	22	20	20.04	2.60±0.84	5.80±1.82
	15.5	40	16.23	1.99±0.35	7.15±1.50
	10	40	11.05	1.47±0.36	11.35±3.27
	6.5	20	8.19	0.51±0.18	7.38±3.57

Note: Values are mean ± 95% confidence interval (CI). n is the number of particles tested in each size class; d is the measured mean particle diameter; F_{max} is the maximum crushing force; σ is the fracture strength. The same 95% CIs are the uncertainty measure used throughout the text.

3.1.1. Maximum crushing force and particle size

To elucidate the patterns of particle fragmentation behavior, we analyzed the mechanical responses and statistical characteristics under various particle size and mineral composition conditions. The results of the single-particle uniaxial compression tests are shown in Fig. 2 Different minerals exhibit a distinct size effect across all particle size ranges. As particle size increases, the maximum crushing force tends to rise, while the corresponding uniaxial compressive strength gradually decreases. Although the trends of these two parameters are opposite, they follow clear statistical patterns. The regression results indicate that the coefficients of determination (R^2) for all mineral samples exceed 0.98, demonstrating that the power-law relationship effectively describes the dependence of maximum breakage force on particle size. The high correlation coefficients confirm a stable relationship between overall load-bearing capacity and particle size. With increasing particle size, both the effective load-bearing volume and

contact area increase, thereby enhancing the load-bearing capacity of the particle. Consequently, a greater external force was required to initiate failure, resulting in an increase in the maximum breakage force.

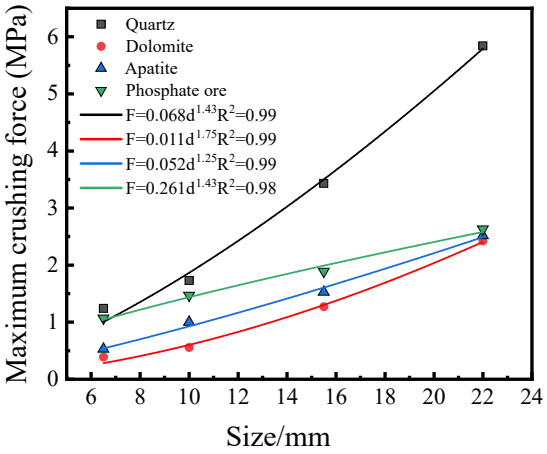


Fig. 2. Relationship between maximum crushing force and particle size. Symbols aremeans (n - 20). For clarity, error bars are not shown; the 95% confidence intervals are listed in Table 1. Dashed linesare power-law fits ($F = a*d^b$)

3.1.2. Breaking strength and particle size

After converting the maximum breakage force into compressive strength, a typical inverse size effect is observed, whereby strength decreases with increasing particle size (see Fig. 3). This phenomenon is associated with the statistical distribution of internal defects within particles. Larger particles are more likely to contain microcracks, structural discontinuities, and mineral interfaces, which act as stress concentrators during loading. As a result, cracks initiate more easily and propagate at lower stress levels, leading to a reduction in macroscopic strength. The size effect (Crain, 2011) is reflected not only in the average strength level but also in the stability of breakage behavior, providing a basis for subsequent statistical analysis.

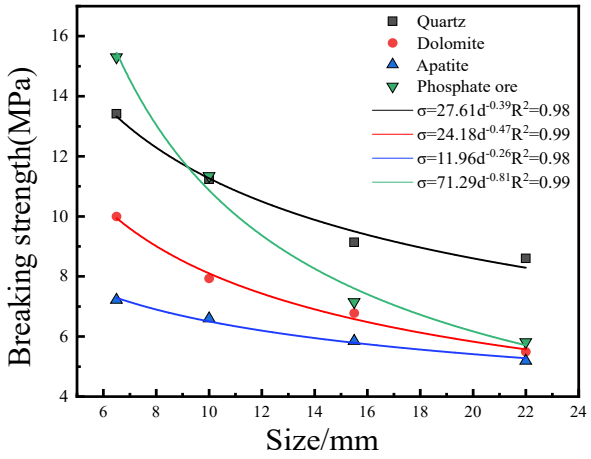


Fig. 3. Compressive strength as a function of particle size. Symbols aremeans (n - 20). For clarity, error bars are not shown; the 95% confidence intervals are listed in Table 1. Dashed linesare power-law fits ($F = a*d^{-b}$)

3.1.3. The effect of multi-component structures on crushing behavior

Building on the analysis of size effects, this study further examines the influence of differences in mineral composition on crushing behavior. Under identical particle size conditions, multi-component phosphate ore exhibits markedly different crushing characteristics compared to pure minerals. Overall, the maximum crushing force of phosphate ore is generally higher than that of pure apatite, and the trends in strength vary from those of pure minerals. Within a narrower particle size range, the compressive strength of phosphate ore can exceed that of some pure minerals.

The difference in strength between multi-component phosphate ore and pure minerals is shown in Fig. 4 The fracture strength of both apatite and phosphate ore decreases with increasing particle size, but the decrease in phosphate ore is more pronounced, dropping from 15 MPa to 6.5 MPa; in contrast, the decrease in apatite is approximately 2.5 MPa. this phenomenon is related to the multi-mineral embedding structure. High-strength minerals such as quartz and dolomite form local load-bearing frameworks that constrain weaker mineral phases, thereby improving the local load-bearing capacity. Meanwhile, cracks deflect at the interfaces between different minerals, thereby lengthening the propagation path and increasing the energy required for failure. Consequently, the overall resistance to fracture is enhanced. As particle size increases, the influence of the multi-component structure gradually shifts. intra-particle heterogeneity becomes more pronounced and the number of mineral interfaces increases (Zhu et al., 2008; Wang, Li, Wang, Li, Wang, Feng, Fu, 2024; YANG, J., LI, Y., ZHU, P., LI, Z., LI, H., MA, S., 2024), which in turn creates additional sites for crack initiation and propagation. As a result, microcracks gradually become the dominant factor controlling failure, resulting in a more pronounced reduction in strength. The decline in strength with decreasing particle size is more pronounced in multi-component ores, and the difference between them and pure minerals gradually widens. This indicates that the mechanisms by which multi-mineral embedded structures influence fracture behavior differ across scales: at small scales, they manifest as structural reinforcement, whereas at large scales, they manifest as defect-dominated behavior (ZHANG, D.H., ZHU, F.S., XING, J.B., YANG, S.C., 2005; Astrom, 2006).

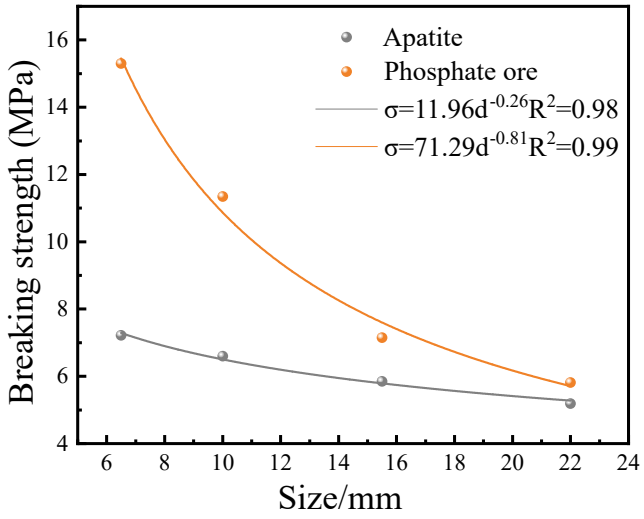


Fig. 4. Fracture strength as a function of particle size for apatite and phosphate ore. For clarity, error bars are not shown; the 95% confidence intervals are listed in Table 1. Dashed linesare power-law fits ($F = a*d^{-b}$)

The failure characteristics of multi-component phosphate ore are governed by the interaction between size effects and structural heterogeneity. Experimental observations reveal that both the characteristic strength (σ_0) and Weibull modulus (m) vary systematically with particle size, indicating that these parameters are better interpreted as evolving statistical descriptors rather than intrinsic material constants.

3.2. Strength statistical characteristics and Weibull parameters

3.2.1. Two-parameter Weibull distribution

Data on fracture strength and particle-size distribution were compiled of 320 samples of four types of irregular ore during catastrophic failure; the results are shown in Table 2 There is significant variability between fracture strength and particle size distribution for these irregular ores. Given this variability in the experimental data, statistical methods are required to analyze and characterize the fracture strength characteristics of the four types of irregular ore.

Particle breakage strength exhibits significant dispersion, and a single average value cannot adequately represent its mechanical characteristics. According to the weakest link theory, failure in

brittle materials is governed by the most critical flaw, and the strength distribution can be effectively described using the Weibull model. In the two-parameter Weibull distribution, the characteristic strength σ_0 represents the overall strength level of the material, while the modulus m reflects the degree of dispersion in the strength distribution (see Fig. 5). The results indicate that the Weibull model

Table 2. Weibull parameter statistics

Size	Ore	m	σ_0/MPa	R^2
-25+19mm	Quartz	2.329	10.162	0.821
	Dolomite	2.434	6.243	0.971
	Apatite	1.477	5.144	0.950
	Phosphate ore	1.992	6.465	0.900
-19+12mm	Quartz	2.371	10.369	0.967
	Dolomite	1.695	7.569	0.992
	Apatite	2.171	6.318	0.967
	Phosphate ore	1.983	7.965	0.973
-12+8mm	Quartz	2.329	12.614	0.929
	Dolomite	1.484	8.703	0.913
	Apatite	1.900	7.704	0.967
	Phosphate ore	1.534	12.137	0.926
-8+5mm	Quartz	2.865	15.112	0.942
	Dolomite	1.895	11.134	0.907
	Apatite	1.355	8.190	0.857
	Phosphate ore	1.950	16.926	0.912

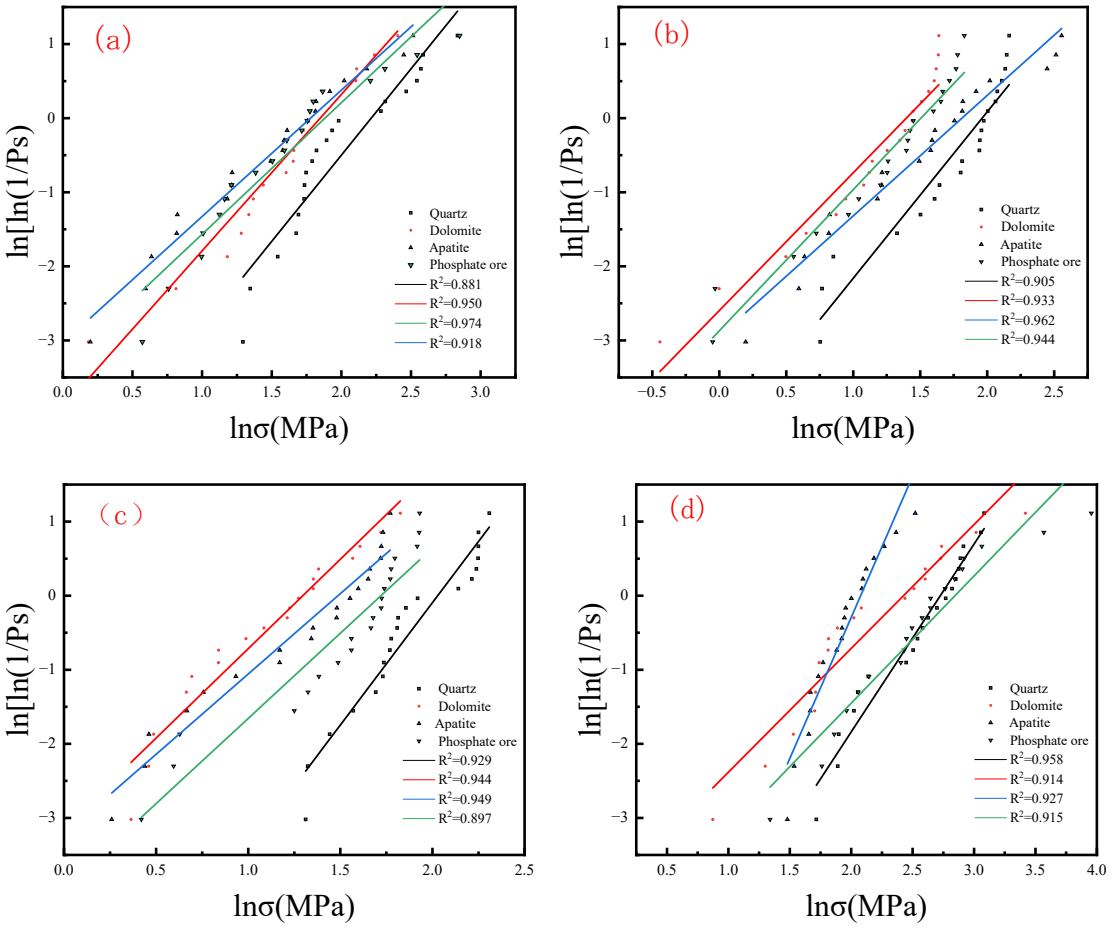


Fig. 5. Weibull fitting plots for different ores at various particle sizes: (a) 25–19 mm, (b) 19–12 mm, (c) 12–8 mm, and (d) 8–5 mm

provides a good description of the particle strength distribution characteristics. The degree of strength dispersion varies markedly across particle size ranges. The 25–19 mm fraction exhibits the highest concentration of strength values and the lowest variability, whereas the 12–8 mm fraction shows a broader distribution and greater scatter. Such differences suggest that particle failure is governed by the combined influence of size-dependent effects and internal structural characteristics. Variations in particle size alter the relative contributions of mineral boundaries, microcracks, and inherent defects during crack initiation and propagation. Consequently, the fracture process evolves with particle size, leading to distinct strength distribution patterns and different Weibull parameters among particle-size fractions. As a result, the statistical distribution of particle strength evolves with size, leading to distinct strength distribution patterns among different size fractions.

3.2.2. Discrete characterization of strength

Fig. 6 illustrates the evolution of the Weibull modulus (m) for different mineral specimens across several particle size ranges. Variations in m are observed among the tested size fractions; however, no consistent monotonic relationship with particle size is evident. The contrast between pure minerals and phosphate ore is more pronounced than the influence of particle size alone. In general, pure mineral specimens exhibit higher m values. Notably, apatite in the 8–5 mm size fraction attained an m value of 3.81, reflecting a relatively narrow strength distribution and a more predictable failure response. By comparison, the m values of phosphate ore remained within the range of 1.72–2.30, which is lower than those measured for most pure mineral samples. This behavior indicates that the presence of a multi-mineral assemblage introduces additional variability into the fracture process and reduces its stability.

The observed differences can be attributed to the combined effects of mineral interfaces, inherent structural defects, and contrasts in mechanical properties among constituent minerals. These factors alter crack initiation and propagation behavior, resulting in more tortuous fracture paths and greater dispersion in particle strength, thereby reducing the Weibull modulus (m) and increasing the uncertainty of fracture behavior. The findings further suggest that the Weibull modulus m responds more strongly to structural heterogeneity than to particle size variation. Consequently, m provides an effective statistical parameter for describing the stochastic nature of failure in multi-component ore systems.

In summary, the size effect primarily influences σ_0 by altering the strength level, while structural heterogeneity primarily affects the m-value, causing it to reflect the uncertainty inherent in the fracture process (Bai, Li, Feng, Liu, Gao, Zhang, Nie, 2023). he Weibull parameters provide a unified description of strength in terms of its discrete characteristics to a certain extent.

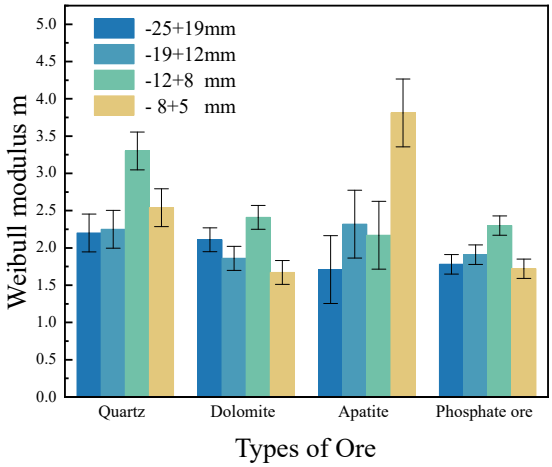


Fig. 6. Comparison of Weibull modulus m of different ores. Error bars represent the standard deviation (± SEM)

A pronounced size dependence can be observed for all materials. When particle size increased from 6 mm to 10 mm, σ_0 decreased markedly across all samples, highlighting the dominant influence of the size effect on particle strength. Beyond this range, the evolution of σ_0 became more complex. Quartz, dolomite, and phosphate ore exhibited varying degrees of recovery in characteristic strength, whereas

apatite displayed only minor fluctuations. Such behavior indicates that, under coarser particle size conditions, strength evolution cannot be explained solely by the size effect (He, 2019; Li, Xiao, Fu, Jin, Wang, Wang, Sun, Tian, Liu, Tian, 2025).

The distinct responses observed among different minerals further suggest that characteristic strength is influenced not only by particle size but also by mineralogical composition, interfacial characteristics, and the spatial distribution of internal defects. In the case of multi-component phosphate ore, the presence of high-strength mineral phases can generate localized load-bearing frameworks at smaller particle sizes, thereby improving the overall resistance to failure. As particle size increases, however, the degree of structural heterogeneity becomes more significant. The increased number of mineral interfaces and defects promotes crack initiation and propagation, thereby reducing the effective load-bearing capacity and contributing to the decline of σ_0. Mineral interfaces and pre-existing microcracks exert a stronger influence on crack initiation and propagation, promoting failure and contributing to the reduction of σ_0.

These findings demonstrate that characteristic strength σ_0 should not be regarded as an intrinsic material constant (Ngo et al., 2001; Qi, Ju, Yu, Meng, Qiao, 2022; Yin et al., 2023). Instead, it represents a statistical parameter that evolves under the coupled influence of size-dependent effects and structural heterogeneity.

For the constituent minerals, the size-effect exponent fitted with Eq. (4) is b = 0.35, 0.47 and 0.42 for quartz, dolomite and apatite, respectively, whereas the composite phosphate ore gives b = 0.82. The corresponding products b·m are 0.85, 0.88, 0.72 and 1.52 (mean ≈ 1.0). The −1/m scaling in Eq. (3) requires b·m = 1, whereas the −3/m form would require b·m = 3; the observed values therefore support the former and are incompatible with the latter. The phosphate ore shows the largest b·m, indicating that its size effect is stronger than predicted from the Weibull modulus alone, which is consistent with the additional weakening provided by interphase boundaries, microcracks and fine intergrowth in the multi-mineral assemblage. In contrast, the Weibull modulus itself shows no systematic trend with particle size (Fig. 6), whereas the characteristic strength decreases consistently with size (Fig. 7). The four materials also differ in absolute strength and in the steepness of their strength–size curves. Quartz shows the highest absolute strength and the weakest size dependence, which is consistent with its ordered silicate framework and low defect density; apatite shows the lowest absolute strength, consistent with its finer crystallites and higher defect density; dolomite lies between these two. The composite phosphate ore exhibits the steepest decline with increasing size: at small sizes its rigid quartz/dolomite framework confines crack growth and raises the strength, whereas at large sizes the growing number of phase boundaries and microcracks makes fracture progressively easier.

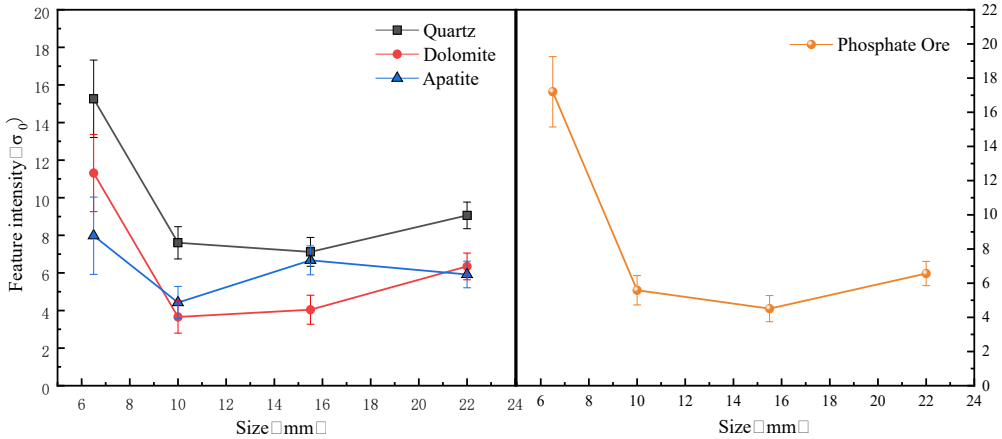


Fig. 7. σ_0 curves of different ore particle sizes and characteristic strengths: (a) relationship curves for pure minerals, (b) relationship curves for phosphate ore. Error bars represent the standard deviation (± SEM)

3.3. Analysis of crushing mechanism

As particle size increases, heterogeneity effects in multi-mineral systems become increasingly pronounced (Wang, He, Hu, Li, Ma, Ren, 1981; Yapei et al., 2024; Wang, He, Hu, Li, Ma, Ren, 2026).

Mechanical differences between different minerals lead to local stress redistribution and the formation of non-uniform stress fields. As a result, the fracture process becomes more random. This behavior is reflected in a decrease in the Weibull modulus (m), indicating a broader strength distribution and higher variability (MATTYASOVSZKY-ZSOLNAY, 1957;Liu, Zhao, Tang, Liao, Wang, Tan, Chang, Luo, Wang, 2022; Feng, Cao, Li, Tang, Li H.-J., 2023). Therefore, the decrease in m can be directly attributed to the increased complexity of crack propagation in multicomponent structures.

From a micro perspective, Grain size and defect distribution characteristics indirectly govern grain strength and its variability by affecting crack initiation behavior. the XRD analysis results (see Fig. 8) provide further evidence for the mechanical differences observed. Quartz exhibits sharp and narrow diffraction peaks with high intensity, indicating an ordered crystal structure and relatively low defect density (Marshall and Cox, 1987; Dittmer, Ritzberger, Schweiger, Rheinberger, Wörle, Höland, 2014; He, Chen, Wang, Wei, Chen, 2018), which in turn contributes to a more stable fracture response. In addition, the crystallite size is relatively large. However, the apatite exhibits multiple broad and widely dispersed diffraction peaks, indicating small grain sizes and a high defect density, thereby increasing the likelihood of crack initiation. These characteristics imply lower structural uniformity and greater variability in mechanical response. However, diffraction peak morphology alone cannot fully characterize the structural heterogeneity of different minerals. Therefore, the Scherrer equation was further applied to quantify crystallite size, thereby providing a more direct basis for interpreting the observed differences in fracture behavior. The inverse relationship between diffraction peak broadening and grain size further confirms that grain refinement is generally accompanied by an increase in defect density. As a result, finer grains provide additional crack initiation sites and promote more heterogeneous fracture behavior. Although grain refinement may enhance strength under certain conditions, the accompanying increase in defect density also increases the stochasticity of crack initiation and propagation.

This interpretation is generally consistent with the trend observed in Fig. 7, further demonstrating that mineral structure and interfacial effects jointly govern particle fragmentation behavior in multicomponent ores. The crystallite sizes calculated using the Scherrer equation (Guo, Qi, Zou, Zheng, 2017) are presented below, and the corresponding expression is given in Eq. (11):

$$D=\frac{K\lambda}{\beta \cos\theta} \tag{11}$$

Here, D represents the grain size, K is the shape factor (taken as 0.89), λ is the X-ray wavelength (taken as 1.5406 nm), β is the half-width of the diffraction peak in radians, and θ is the diffraction angle (°); these values are used to estimate the size of the powder crystals.

As shown in Table 3 the diffraction peak at 20.858° corresponds to the quartz phase, the peak at 26.642° corresponds to the dolomite phase, and the peak at 31.999° corresponds to the apatite phase. According to the Scherrer formula, the crystal diameter of SiO_2 in the quartz powder is 54–68 nm, that of $CaMg(CO_3)_2$ in the dolomite powder is 48–52 nm, and that of $Ca_5(PO_4)_3$(F, Cl, OH) in the apatite powder is 20–34 nm. Phosphate ores contain tetrahedral, rhombohedral, and hexagonal crystal systems that together form a highly heterogeneous multi-mineral assemblage. The substantial differences in crystallite size among these mineral phases imply variations in crystal integrity and defect distribution. Consequently, stress redistribution and crack deflection are more likely to occur at mineral interfaces, resulting in greater variability in fracture behavior. These coupled effects jointly influence both the characteristic strength (σ_0) and the Weibull modulus (m), producing fracture responses that differ significantly from those of single-mineral systems (Snyder, Fiala, Bunge, 1999). Analysis based on the Weibull distribution demonstrates that σ_0 primarily represents the general strength level of the material, whereas m is closely associated with structural heterogeneity and the degree of dispersion in fracture responses. In addition, crystallographic information derived from the Scherrer equation suggests that grain size and defect density contribute indirectly to fracture behavior through their influence on crack initiation and growth.

To illustrate more clearly the differences in fracture patterns between single-mineral and multi-mineral ores (see Fig. 9), as shown in Fig. 9 (a), in pure mineral grains, the internal structure is relatively uniform; cracks often originate from local defects and propagate along the direction of maximum principal stress, thereby forming relatively simple and nearly linear paths. Consequently, the fracture

paths remain relatively regular, the failure modes are relatively simple, and the strength distribution is relatively concentrated. This behavior is consistent with the higher Weibull modulus observed in most pure mineral samples.

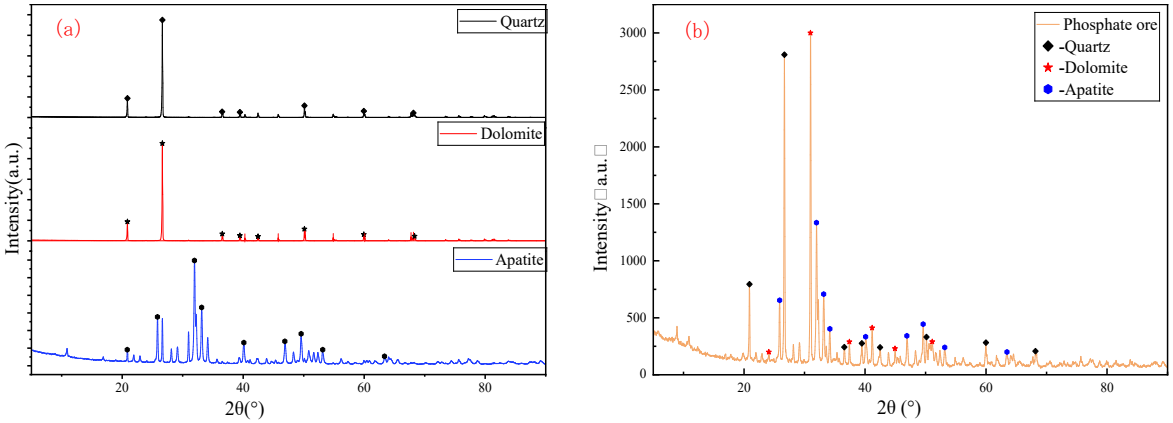


Fig. 8. XRD patterns of (a) pure minerals and (b) phosphate ore

Table 3. Diffraction peak parameters of different grains

Crystal type	2θ/°	cosθ	Diffraction peak widening β/radian	D/nm
Silicon-oxygen tetrahedral crystal form	20.858	0.983	0.00203	54
	39.470	0.941	0.00265	68
Rhomboid crystal type	26.642	0.973	0.00267	52
	50.147	0.905	0.00314	48
Hexagonal crystal system	31.999	0.961	0.00694	20
	33.142	0.958	0.00411	34

In contrast, phosphate rock exhibits fracture characteristics typical of a multi-component ore structure, consisting of quartz, dolomite, and apatite. The coexistence of minerals with different crystal structures, grain sizes, and mechanical properties results in significant structural heterogeneity. The substantial differences in crystal size among the constituent minerals indicate variations in crystal integrity and defect distribution. Finally, under external loading, stress redistributes at mineral interfaces due to mismatches in elasticity and strength between adjacent phases. As shown in Fig. 9 (b), As particle size increases, the influence of mineral interfaces becomes increasingly significant. Larger particles contain more mineral boundaries and structural discontinuities, providing additional sites for crack initiation and propagation. Consequently, crack paths become increasingly complex and unpredictable, resulting in a broader strength distribution and lower Weibull modulus values. Fractures occur along the original mineral interfaces, and new mineral interfaces form along the resulting cracks,

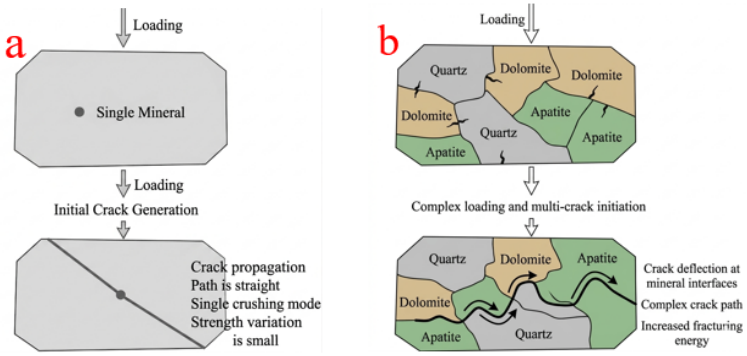


Fig. 9. Schematic illustration of the mechanism by which multi-mineral embedded structures influence particle fracture behavior: (a) Fracture patterns of pure mineral particles, (b) Fracture patterns of multi-mineral embedded ore

eventually giving rise to new combinations of mineral interfaces. Consequently, the fracture process becomes more random, resulting in a broader strength distribution and lower Weibull modulus values.

The observed fracture behavior indicates that particle fracture in pure minerals is primarily governed by the intrinsic properties of the minerals, whereas fracture in multicomponent phosphorites is jointly controlled by mineralogical heterogeneity, interfacial effects, and defect mechanisms.

A comprehensive analysis indicates that particle fracture in multi-mineral systems is influenced by a combination of size effects and structural heterogeneity. An increase in particle size is accompanied by a higher probability of defect occurrence within the particle, which facilitates crack nucleation and subsequent propagation, ultimately reducing the overall fracture strength. Meanwhile, the coexistence of quartz, dolomite, and apatite creates numerous mineral interfaces that alter local stress transmission and increase the tortuosity of crack trajectories. As a result, the fracture process becomes more complex and exhibits greater variability. Size effects control the overall strength level through defect accumulation, while heterogeneity affects the variability of fracture behavior by altering the crack propagation path (Bunaciu et al., 2015; Khelifi et al., 2024; Shen et al., 2025). These two mechanisms are inherently coupled and jointly determine the characteristic strength (σ_0) and the Weibull modulus (m). The entire process is described within a unified framework encompassing defect evolution, crack propagation, and statistical response (Evans, Dalgleish, He, Hutchinson, 1989; Martínez-Pañeda et al., 2019; North China University of Science and Technology Researchers, 2022). This framework provides a coherent explanation for the trends in strength and Weibull parameters observed experimentally and highlights the fundamental differences between single-mineral and multi-mineral systems (Lu et al., 1999; Nelson, 2010). Such findings provide a theoretical basis for fracture modeling and improve the understanding of scale-dependent strength characteristics in complex ores. The combined effects of particle size and structural heterogeneity govern the evolution of strength distribution and failure mechanisms in multicomponent phosphate ores, providing valuable insights for crushing modeling and characterizing the scale dependence of ore strength.

3.4. Scope and limitations

This study is concerned with the mechanical response of single particles—the maximum crushing force, the fracture strength and its Weibull statistics—and with how these properties scale with particle size and mineralogy. The experiments were therefore designed to quantify breakage resistance rather than the fragmentation outcome. Accordingly, the size distribution of the breakage products, and particularly the yield of the −5 mm fraction, was not determined in the present experimental programme. Characterizing the product size distribution requires sieving and weighing of the fragments produced in each test, which is a distinct characterization and is addressed in a follow-up study. It is nevertheless worth noting that heterogeneous, multi-mineral ores have been reported to generate more fines at a given specific energy (Lois-Morales et al., 2022), which is qualitatively consistent with the lower strength and greater structural heterogeneity observed here for the composite phosphate ore.

4. Conclusions

To investigate the influence of ore structure and composition on the crushing behavior of multi-component ores, this study employs uniaxial compression tests and incorporates the Weibull model to analyze the ore crushing process under various conditions. Concurrently, a comparative study was conducted on the strength characteristics of pure minerals and actual ores under different particle size conditions, as well as the structural heterogeneity reflected by the Weibull distribution. This approach not only provides theoretical support for mechanistic analysis but also lays a solid foundation for elucidating the fracture behavior of ores under varying particle size conditions. The main conclusions of this paper are as follows:

(1) A pronounced size effect was observed in the tested materials, with particle strength decreasing as particle size increased. Compared with pure minerals, multi-component ores exhibited a more substantial reduction in strength, suggesting that structural heterogeneity amplifies the influence of particle size on mechanical behavior.

(2) The failure response of multi-component ores was found to be strongly dependent on particle size. In finer particle fractions, the embedded mineral framework provided structural confinement that restricted crack development. As particle size increased, the influence of internal defects became progressively more significant, and fracture behavior transitioned toward a defect-dominated regime.
(3) The Weibull distribution was capable of capturing the statistical variability of particle strength. The characteristic strength σ_0 showed a declining trend with increasing particle size, whereas the Weibull modulus m remained consistently lower in multi-component ores and generally decreased further at larger size fractions. These observations indicate that Weibull parameters evolve with scale and should not be regarded as invariant material properties.
(4) The size effect and structural heterogeneity jointly govern the fracture mechanism of particles. Size variations modulate the strength σ_0 by influencing the number of defects, while the multi-mineral embedded structure affects m by altering the complexity of crack paths; the coupling of these two factors gives rise to the strength and dispersion characteristics unique to multicomponent ores.

Acknowledgments

This research was funded by National Engineering and Technology Research Center for Development &Utilization of Phosphate Resources (NECP-2024-02) and Yunnan Fundamental Research Projects (No. 202501CF070273).

References

ALONA N., DANIEL S., 2018. *Comparative analysis of the strength distribution for irregular particles of carbonates, shale, and sandstone ore.* Minerals 8, 37.

ARMSTRONG R.W., 2019. *Size effects on material yield strength/deformation/fracturing properties.* J. Mater. Res. 34, 1–16.

ASTROM J.A., 2006. *Statistical models of brittle fragmentation.* Advances in Physics 55(3–4).

BAI J., LI C., FENG R., et al., 2023. *Effect of water content on the impact propensity of white sandstone.* Geofluids 2023, 8839852. https://doi.org/10.1155/2023/8839852.

BERTALAN Z., SHEKHAWAT A., SETHNA J.P., et al., 2014. *Fracture strength: stress concentration, extreme value statistics, and the fate of the Weibull distribution.* Phys. Rev. Appl. 2, 034008.

BUDEMBERG G., JOLSTERÅ R., CHEHREH CHELGANI S., 2025. *Eco-friendly collectors in apatite froth flotation: a review.* Int. J. Miner. Sci. Technol. 35, 539–551.

BUNACIU A.A., UDRIȚIOIU E.G., ABOUL-ENEIN H.Y., 2015. *X-ray diffraction: instrumentation and applications.* Crit. Rev. Anal. Chem. 45, 289–299.

CHEN Y., ZHANG J., XIONG C., et al., 2026. *Efficiency and mechanism of malonic acid as a depressant in the reverse flotation separation of apatite from dolomite.* Colloids Surf. A 748, 141073.

CRAIN M.A., 2011. *A literature review of the size effect.* Social Science Electronic Publishing. https://doi.org/10.2139/ssrn.1710076.

DITTMER M., RITZBERGER C., SCHWEIGER M., et al., 2014. *Phase and microstructure formation and their influence on the strength of two types of glass-ceramics.* J. Non-Cryst. Solids 384, 55–60.

DYSKIN A.V., PASTERNAK E., 2020. *Discrete self-similarity of multiscale materials and systems. Universality of scaling exponents.* Int. J. Eng. Sci. 149, 103244.

EVANS A.G., DALGLEISH B.J., HE M., et al., 1989. *On crack path selection and the interface fracture energy in bimaterial systems.* Acta Metall. 37, 3249–3254.

FENG P., CAO P., LI J., et al., 2024. *Dynamic fracture mechanism and fragment characteristics of sandstone specimens with asymmetrical conjugate fissures under static pre-compression.* Sci. Rep.

GUO S., QI S., ZOU Y., et al., 2017. *Numerical studies on the failure process of heterogeneous brittle rocks or rock-like materials under uniaxial compression.* Materials 10, 378.

HE K., CHEN N., WANG C., et al., 2018. *Method for determining crystal grain size by X-ray diffraction.* Cryst. Res. Technol. 53, 1700157.

HE K.L.M., 2019. *Effects of clay content, cement and mineral composition characteristics on sandstone rock strength and deformability behaviors.* J. Pet. Sci. Eng. 176.

HIRAMATSU Y., OKA Y., 1966. *Determination of the tensile strength of rock by a compression test of an irregular test piece.* Int. J. Rock Mech. Min. Sci. Geomech. Abstr. 3, 89–99.

HUKKI R.T., 1961. *Proposal for a solomonic settlement between the theories of von Rittinger, Kick and Bond.* Trans. AIME 220, 403–408.

JINLIN Y., YUAN L.I., PENGYAN Z., et al., 2024. *Study on grinding characteristics of multi-component complex ore and its component minerals under dropping grinding.* Nonferrous Met. (Miner. Process. Sect.) 11.

KHELIFI S., AYAD A., BOUMAIZA A., et al., 2024. *Correlations between XRD peak broadening and elastic and plastic deformation for mild steel sheets under tensile loading.* Mater. Sci. (Medžiagotyra) 30.

KLEIN C., 2007. *The manual of mineral science.*

LI Y., XIAO Q., FU Y., et al., 2010. *An innovative theoretical model for optimizing ball diameter in tumbling mills.* Miner. Eng. 233, 109635. https://doi.org/10.1016/j.mineng.2025.109635.

LIU Q., ZHAO Y., TANG L., et al., 2022. *Mechanical characteristics of single cracked limestone in compression-shear fracture under hydro-mechanical coupling.* Theor. Appl. Fract. Mech. 119, 103371.

LOIS-MORALES P., EVANS C., WEATHERLEY D., 2022. *Analysis of the size-dependency of relevant mineralogical and textural characteristics to particles strength.* Miner. Eng., 107572.

LU C., VERE-JONES D., TAKAYASU H., 1999. *Avalanche behavior and statistical properties in a microcrack coalescence process.* Phys. Rev. Lett. 82, 347–350.

MARSHALL D.B., COX B.N., 1987. *Tensile fracture of brittle matrix composites: influence of fiber strength.* Acta Metall. 35, 2607–2619.

MARTÍNEZ-PAÑEDA E., FUENTES-ALONSO S., BETEGÓN C., 2019. *Gradient-enhanced statistical analysis of cleavage fracture.* Eur. J. Mech. A/Solids 77, 103785.

MATTYASOVSZKY-ZSOLNAY L., 1957. *Mechanical strength of porcelain.* J. Am. Ceram. Soc. 40. https://doi.org/10.1111/j.1151-2916.1957.tb12626.x.

NELSON W.B., 2010. *Defect initiation, growth, and failure – a general statistical model and data analyses.* Birkhäuser Boston. https://doi.org/10.1007/978-0-8176-4924-1_3.

NGO A.T., BONVILLE P., PILENI M.P., 2001. *Spin canting and size effects in nanoparticles of nonstoichiometric cobalt ferrite.* J. Appl. Phys. 89, 3370–3376.

NORTH CHINA UNIVERSITY OF SCIENCE AND TECHNOLOGY *researchers describe research in mineral research (The meso-structural characteristics of crack generation and propagation during rock fracturing).*, 2022. Mining & Minerals Daily, February 4.

QI Y., JU Y., YU K., et al., 2022. *The effect of grain size, porosity and mineralogy on the compressive strength of tight sandstones: a case study from the eastern Ordos Basin, China.* J. Pet. Sci. Eng. 208, 109461.

SHEN L., ZHANG H., HAO Y., 2025. *Effect of mineral materials heterogeneity on rock failure: insights from a uniaxial compressive test of sandstone by in-situ X-ray computed tomography.* Sci. Rep. 15.

SNYDER R.L., FIALA J., et al., 1999. *Defect and microstructure analysis by diffraction.*

SOMANI A., NANDI T.K., PAL S.K., et al., 2017. *Pre-treatment of rocks prior to comminution – a critical review of present practices.* Int. J. Miner. Sci. Technol. 27.

TAVARES L.M., 2022. *Review and further validation of a practical single-particle breakage model.* KONA Powder Part. J. 39, 62–83.

TIAN M., ZHANG C., ZHU L., et al., 2026. *A novel sulfinyl-containing carboxylic acid collector in synergy with sodium alginate inhibitor for the selective direct flotation separation of apatite from dolomite.* Appl. Surf. Sci. 725, 165820.

UNLAND G., AL-KHASAWNEH Y., 2009. *The influence of particle shape on parameters of impact crushing.* Miner. Eng. 22, 220–228.

WANG W., HE M., HU J., et al., 2026. *Effect of bedding structure and homogeneity on the shale failure: insights from Weibull-based discrete element method (DEM) modeling.* Int. J. Numer. Anal. Methods Geomech. 50, 1697.

WANG Z., SONGYU L.I., WANG J., et al., 2024. *Evolution mechanism and quantitative characterization of initial micro-cracks in marble under triaxial compression.* J. Zhejiang Univ. Sci. A 25, 586–595.

WEIBULL W., 1951. *A statistical distribution function of wide applicability.* J. Appl. Mech. 18, 293–297.

YANG B., LI J., HE J., et al., 2026. *Selective adsorption and surface wettability modulation of quartz by amide-based gemini collector GS-A6 for efficient apatite–quartz reverse flotation.* Appl. Surf. Sci. 730, 166340.

YANG S.Q., LI K.S., SUN B.W., et al., 2025. *Experimental study on the mechanical behavior and fracturing mechanism of red sandstone under triaxial monotonic and multilevel cyclic loading.* Rock Mech. Rock Eng. 58, 11819–11841.